NEURAL REGENERATION RESEARCH
April 2016, Volume 11, Issue 4
www.nrronline.org

RESEARCH ARTICLE

Cell proliferation and apoptosis in optic nerve and brain integration centers of adult trout *Oncorhynchus mykiss* after optic nerve injury

Evgeniya V. Pushchina[1, *], Sachin Shukla[2], Anatoly A. Varaksin[1], Dmitry K. Obukhov[3]

1 Laboratory of Cytophysiology, A.V. Zhirmunsky Institute of Marine Biology Far Eastern Branch of Russian Academy of Sciences, Vladivostok, Russia
2 Prof. Brien Holden Eye Research Centre, L.V. Prasad Eye Institute, Hyderabad, India
3 St. Petersburg State University, Universitetskaya nab. 7/9, St. Petersburg, Russia

How to cite this article: *Pushchina EV, Shukla S, Varaksin AA, Obukhov DK (2016) Cell proliferation and apoptosis in optic nerve and brain integration centers of adult trout Oncorhynchus mykiss after optic nerve injury. Neural Regen Res 11(4):578-590.*

Funding: *This work was supported by a grant from President of Russian Federation (No. MD-4318.2015.4), a grant from Program for Basic Research of the Far East Branch of the Russian Academy of Sciences 2015–2017 (No. 15-I-6-116, section III), and DST-INSPIRE Faculty Grant (No. IFA14-LSBM-104) from the Department of Science and Technology (DST), Government of India.*

Abstract

Fishes have remarkable ability to effectively rebuild the structure of nerve cells and nerve fibers after central nervous system injury. However, the underlying mechanism is poorly understood. In order to address this issue, we investigated the proliferation and apoptosis of cells in contralateral and ipsilateral optic nerves, after stab wound injury to the eye of an adult trout *Oncorhynchus mykiss*. Heterogenous population of proliferating cells was investigated at 1 week after injury. TUNEL labeling gave a qualitative and quantitative assessment of apoptosis in the cells of optic nerve of trout 2 days after injury. After optic nerve injury, apoptotic response was investigated, and mass patterns of cell migration were found. The maximal concentration of apoptotic bodies was detected in the areas of mass clumps of cells. It is probably indicative of massive cell death in the area of high phagocytic activity of macrophages/microglia. At 1 week after optic nerve injury, we observed nerve cell proliferation in the trout brain integration centers: the cerebellum and the optic tectum. In the optic tectum, proliferating cell nuclear antigen (PCNA)-immunopositive radial glia-like cells were identified. Proliferative activity of nerve cells was detected in the dorsal proliferative (matrix) area of the cerebellum and in parenchymal cells of the molecular and granular layers whereas local clusters of undifferentiated cells which formed neurogenic niches were observed in both the optic tectum and cerebellum after optic nerve injury. *In vitro* analysis of brain cells of trout showed that suspension cells compared with monolayer cells retain higher proliferative activity, as evidenced by PCNA immunolabeling. Phase contrast observation showed mitosis in individual cells and the formation of neurospheres which gradually increased during 1–4 days of culture. The present findings suggest that trout can be used as a novel model for studying neuronal regeneration.

Key Words: *nerve regeneration; proliferation; apoptosis; optic nerve; brain; radial glia cells; neurogenic niches; neurospheres; neural regeneration*

***Correspondence to:**
Evgeniya V. Pushchina, D.Sc., Ph.D., puschina@mail.ru.

orcid:
0000-0003-0388-3147 (Evgeniya V. Pushchina)

doi: *10.4103/1673-5374.180742*
http://www.nrronline.org/

Accepted: *2015-12-22*

Introduction

It is known that among vertebrates, fishes are able to effectively rebuild the structure of cells and fibers after central nervous system injury. This concerns both the ability to restore the number of damaged cells through the production of new cells in the matrix areas and neurogenic niches of the brain, and the ability to restore the structure of the axons of injured neurons. However, there are only little data available on how repair process is related to neurogenesis in the adult brain (Kishimoto et al., 2012), and what elements of the proliferative areas of the brain are involved in fish reparative neurogenesis. In order to address this issue, we investigated the changes in the cellular composition of the proliferative areas of the brain in response to damaging effects of the eyes (mechanical damage to the retina and optic nerve) in adult trout.

Optic nerve injury often induces massive nerve cell death and irreversible visual functional impairment in mammals, such as cat (Watanabe et al., 2001), rabbit (Germain et al., 2004), and mouse (Bonfanti et al., 1996). Lower vertebrates, like zebrafish (Zou et al., 2013), *Rana pipiens* (Scalia et al., 1985) and *Litoria moorei* (Humphrey and Beazley, 1985), however, can recover visual function due to survival of retinal ganglion cells (RGCs). In goldfish, about 90% of RGCs survive and rapidly regrow axons to the optic tectum about 2 weeks after axotomy (Rodger et al., 2005). Fish has excellent potential to regenerate RGC axon to the optic tectum within 5 days after optic nerve crush (Wyatt et al., 2010). It can restore visual function, compared with 16 weeks for sunfish (Callahan and Mensinger, 2007), 30–50 days for goldfish (Kato et al., 1999) and 40 days for cichlid (Mack,

2007). However, whether RGC survival or neurogenesis is required for visual functional recovery is still a matter of controversy (McCurley and Callard, 2010; Kishimoto et al., 2012). The regenerative ability of the adult brain requires a series of coordinated cellular processes: neuronal progenitor cell proliferation and migration to injury sites, neuronal differentiation, cell survival, and the integration of the new neurons into existing neural circuits. However, the regeneration efficiency of neurons in the injured mammalian brain is extremely low (Arvidsson et al., 2002). In contrast to mammals, the adult central nervous system (CNS) of teleost fish exhibits a high capacity for neuronal regeneration after injury (Zupanc and Sirbulescu, 2013). Thus, comparative studies in zebrafish and mammals should reveal both general and divergent properties of adult neurogenesis.

Here, to investigate the cellular aspects underlying the strong ability of fish to undergo neuronal regeneration, we developed a trout model of adult stab wound injury of eye and optic nerve. Using this model, we tried to reveal a series of regenerative processes in the injured optic nerve and some integration centers of the brain: the optic tectum and the cerebellum. We studied the proliferation of endogenous neuronal progenitor cells in the tectal and cerebellar proliferative zones, the migration of neuronal progenitor cells from the cerebellar matrix proliferative zones towards the injury site, and the proliferative activity of different types of cells both in terms of adult neurogenesis and neurogenic niches. We examined apoptosis in the optic nerve of adult trout (*Oncorhynchus mykiss*) 2 days after injury followed by the proliferative response of cells in the optic nerve and brain integration centers (the optic tectum and the cerebellum) after stab wound injury to the eye. Using morphological analysis and quantification of proportion of proliferating cell nuclear antigen (PCNA)-immunopositive (ip) cells in control and damaged fish, dorsal matrix zone of trout cerebellum and optic tectum was characterized at 1 week after injury of eye. Primary culture of nerve cells from adult trout's brain was established to study the properties of cells in the CNS of adult trout and their proliferative potential *in vitro*. After 4 days of culture, immunohistochemical staining was performed to analyze the proliferative potential of cells in the brain of adult trout. This study was designed to investigate whether adult trout can be used as a novel model for studying neuronal regeneration.

Materials and Methods

Animals

Twenty adult male trout, aged 12–18 months, with body length of 27–36 cm, weighing 271–350 g, were obtained from Ryasan local breeding hatchery, Russia. Trout were raised at 15–17°C with a 14/10-hour light/dark cycle and had a diet once a day. All animal manipulations were conducted in strict accordance with the guidelines and regulations formulated by the Institute of Marine Biology FEB RAS (IMB FEB RAS), Animal Resources Center and Institutional Animal Care and Use Committee, Vladivostok, Russia. The protocol was approved by the Committee on the Ethics of Animal Experiments of the IMB, Vladivostok, Russia.

Immunohistochemical analysis of trout brain and optic nerve injury

Adult trout were anesthetized with tricaine methane-sulfonate (MS-222, Sigma, St. Louis, MO, USA). The cranial cavity of the immobilized fish was perfused with 0.1 M PBS (pH 7.2) containing 4% paraformaldehyde (PFA) solution *via* a syringe. After prefixation, the brain was removed from the cranial cavity and fixed at 4°C for 2 hours in the same solution. Then, the brain was washed five times in 30% sucrose solution at 4°C during 48 hours. Serial frontal transverse brain sections (50 μm thick) of the trout were made using a freezing microtome (Cryo-Star HM 560 MV, Carl Zeiss, Germany).

Optic nerve injury

A sterile 50-gauge needle was inserted into the right eyes of trout to create a 1-cm-deep stab wound. The cornea and mucous membrane, the lens, and the retina were damaged. Using a 50-gauze needle (Carl Zeiss, Oberkochen, Germany), we mechanically destroyed the optic nerve head. **Figure 1** depicts morphological structure and cell apoptosis in the damaged optic nerve. As a result of traumatic effects, the central part of the retina, retinal pigment epithelium, and the optic nerve head with adjacent muscle fiber were destroyed. Contralateral eyes and optic nerve were used as controls. After optic nerve injury, the animals were put into fresh water to recover. Proliferating cell nuclear antigen (PCNA) labeling of optic nerve in the tectum and cerebellum of trout was conducted 1 week after optic nerve injury. The number of PCNA-ip cells in the cerebellum was compared between the optic nerve injured animals and intact animals.

Immunocytochemistry

Immunohistochemical staining (ABC kit) was performed to investigate the proliferative activity of cells in optic nerves and brain of trout after optic nerve injury. PCNA was identified using the standard streptavidin-biotin-peroxidase labeling on free-floating sections. The sections of brain and optic nerve were incubated with mouse anti-PCNA antibody (PC10) (Novus Biologicals, Littleton, CO, USA; 1:3,000) at 4°C for 2 days. For visualization of immunohistochemical labeling, a Vectastain Elite ABC kit (Vector Laboratories, Burlingame, CA, USA) was used. For identification of the reaction products, the substrates of red color (VIP Substrate Kit, Vector Labs, Burlingame, CA, USA) was used. The staining process was controlled under an Axiovert 200M microscope (Carl Zeiss MicroImaging, Göttingen, Germany). The sections were rinsed with water, mounted on slides, dehydrated according to the standard protocol, and embedded in medium BioOptica (Milano, Italy).

Negative control was used to evaluate the specificity of immunohistochemical reaction. Brain sections were incubated for 1 day with 1% nonimmune horse serum rather than primary antibodies and then stained as described above. In all negative control experiments, no immunoreactions occurred.

TUNEL labeling

To reveal apoptotic cells in the optic nerve of trout, we used a technique for immunoperoxidase labeling of fragmented

DNA chains, called terminal deoxynucleotidyl transferase dUTP nick end labeling (TUNEL). After 2-hour fixation in 4% paraformaldehyde based on 0.1 M phosphate buffer (pH 7.2), dissected parts of the optic nerve were washed for 24 hours in 0.1 M phosphate buffer. Then, these samples were put in 30% sucrose solution based on phosphate buffer (0.1 M) for cryoprotection. Horizontal slices (50 μm thick) were prepared using a freezing microtome (Cryo-star HM 560 MV). To identify TUNEL-positive structures, we used an immunoperoxidase identification system, ApopTag Peroxidase In Situ Apoptosis Detection Kit (Chemicon International Inc., Temecula, CA, USA). For blocking endogenous peroxidase, the slices were incubated in 1% hydrogen peroxide for 3 minutes and then washed twice for 5 minutes each in phosphate buffer. The slices were covered with a smoothing buffer (75 μL) and kept for 10 seconds at room temperature. Then the slices were slightly dried, subjected to the action of TdT enzyme (55 μL/5 cm^2), incubated in a humidity chamber for 1 hour at 37°C, and immersed in a blocking buffer for 10 minutes. The slices were washed in phosphate buffer at room temperature three times for 1 minute each, again dried, covered with antidioxygenin conjugate (65 μL/5 cm^2), and incubated in a humidity chamber for 30 minutes. To detect the reaction products, cerebral slices were incubated in the substrate for identification of peroxidase (VIP Substrate Kit; Vector Labs, Burlingame, CA, USA) with control of color development under a microscope, washed three times with phosphate buffer, and mounted on glass slides. The cell nuclei were finally stained with methyl green according to the technique of Brasher (Merkulov, 1969). The preparations obtained were dehydrated using a conventional technique and embedded in medium BioOptica (Milano, Italy). Measurements were made at 400× magnification in five randomly selected fields of view for each area of research. Proliferation index (PI) and apoptotic index (AI) were determined per 1 mm^2 of the slice by the following equations:

$$PI = \frac{\text{Number of PCNA-ip cells} \times 100\%}{\text{Total number of nuclei}}$$

$$IA = \frac{\text{Number of TUNEL-positive cells} \times 100\%}{\text{Total number of nuclei}}$$

Primary culture

Five trout, *Oncorhynchus mykiss* were used in this experiment. The fishes were sacrificed by decapitation and the brain was dissected out aseptically by swabbing the area of interest with 70% alcohol, prior to dissection. The dissected brain and spinal cord were washed in sterile PBS. The tissues were minced with a scalpel into the smallest possible pieces, transferred to a 15 mL sterile tube and washed thrice with PBS. In each wash, the pieces were allowed to settle down and the supernatant was discarded. The tissues were then treated with trypsin (0.25% and 0.025%) and collagenase (28U and 56U) and incubated in water bath for 28°C for 15 minutes (sometimes, a second round of trypsinization was also required to achieve complete disaggregation of the tissues). The trypsinized tissues were transferred to a 50 mL sterile tube and suspended in a complete growth medium (five times to the volume of the trypsin used): Leibovitz's L-15 medium containing 10% fetal bovine serum and 0.4% (v/v) penicillin/streptomycin antibiotic cocktail (Gibco, Gaithersburg, MD, USA/Invitrogen, Carlsbad, CA, USA).

The pieces were disaggregated so as to become single cell suspension. The resulting suspension was allowed to stay in the centrifuge tube for 5 minutes, followed by careful aspiration of the floating cell clumps with the aid of pipette. The suspension was centrifuged at 200 × *g* for 5 minutes, the supernatant was discarded and the pellet was re-suspended in the complete L-15 medium (Gibco, Invitrogen, NY, USA). The resulting cell suspensions from the brain were seeded in the small specially coated duplex dishes and maintained in an incubator at 28°C for 3–4 days for further proliferation and differentiation. The cells were monitored daily and observed under the motorized inverted microscope (Axiovert 200 M, Carl Zeiss, Göttingen, Germany).

Immunocytochemistry of primary culture

To investigate the proliferative properties of the central nervous system of adult trout, *in vitro* culture of primary brain cells was performed, followed by cell culture for 4 days and PCNA expression analysis by immunocytochemical labeling evaluation in cell culture. After 4 days in culture, the cells from brain and spinal cord were processed for immunocytochemistry as per the standard protocol. The suspension and adherent cells (monolayer cells) were processed separately. Briefly, cells grown in suspension were pelleted at 250 × *g* for 5 minutes. Cells in a duplex dish (monolayer population) and suspension fraction were fixed with 4% paraformaldehyde dissolved in phosphate buffer (0.1 M, pH 7.2) for 30 minutes at room temperature. They were washed gently with a stream of PBS. For the inactivation of endogenous peroxidase by an accelerated quenching procedure, cells were incubated with 3% hydrogen peroxide in water for 3–5 minutes and gently washed by PBS. To reduce the background staining, cells were incubated with 1% normal serum in PBS. Thereafter, cells were incubated with primary monoclonal antibody against PCNA (Santa Cruz Biotechnology, Santa Cruz, CA, USA; 1:200) for 1 hour at 37°C, followed by a gentle wash with PBS. They were incubated for 10 minutes with diluted affinity-purified biotinylated secondary antibody (Vectastain Elite ABC kit, Vector Labs, Burlingame, CA, USA) and washed by PBS. Cells were incubated for 5 minutes with Vectastain Elite ABC reagent (Vector Labs, Burlingame, CA, USA) and washed by PBS. Then cells were incubated in peroxidase substrate solution in PBS until stain intensity developed, and washed in PBS. The microscopic analysis was done in duplex dishes under Zeiss Axiovert inverted 200 M microscope (Carl Zeiss, Germany).

Cells from a suspension population were treated with a similar procedure on the poly-L-lysine coated glass slides. After above mentioned procedure of immunocytochemical labeling, cells from suspension fraction were incubated with peroxidase substrate solution for 10 minutes. To identify the reaction products, the slices were incubated in a substrate for detection of peroxidase (VIP Substrate Kit;

Vector Laboratories, Burlingame, CA, USA); the process of staining was controlled under a microscope. Then, the glasses were washed by three changes of phosphate buffer, dried at room temperature, dehydrated using a standard technique, and embedded in medium BioOptica (Milano, Italy). To estimate the specificity of the immunocytochemical reaction, a negative control was used. The cells were incubated in a medium containing 1% nonimmune horse serum (instead of primary antibodies) for 2 hours, and then all procedures were performed as described above. In all negative control experiments, the immunopositivity in the studied cells was absent.

Statistical analysis

For quantitative analyses, all PCNA-ip cells in the tectum opticum and cerebellum were counted under a 40× objective lens using an Axiovert 200 M microscope (Carl Zeiss MicroImaging, Göttingen, Germany). Densitometric investigation of the optical density (OD) of immunolabeled cells was performed using software AxioVision. The OD of immunoprecipitate marked cells was studied on the samples from 50–100 cells. Data are expressed as the mean ± SEM and were analyzed with analysis of variance followed by *post hoc* Tukey's tests unless otherwise stated. P values < 0.05 were considered to be statistically significant. On the basis of morphometric analysis, we allocated five morphological types of cells in accordance with generally accepted neurohistological classification: type I: cells with diameters more than 40 μm; type II: cells with diameters ranging from 20 to 40 μm; type III: cells with diameters ranging from 15 to 20 μm; type IV: cells with diameters ranging from 10–15 μm; and type V: cells with diameters less than 10 μm. Morphometric parameters and the correlations between some of the parameters were analyzed by Microsoft Excel 2010 (Microsoft Office Professional E435-2642, Moscow, Russian Federation).

Results

Cellular response in the optic nerve after injury

Morphological structure and cell apoptosis in the trout optic nerve 2 days after injury: Some morphological characteristics of the injured (ipsilateral) and non-injured (contralateral) trout optic nerves were observed after stab wound of the eye. The morphological structure of trout optic nerve on the contralateral side is shown in **Figure 1A**. In accordance with morphological criteria, four types of cells in damaged and normal optic nerves were identified. The cells were categorized into four types depending upon the size of their diameters (**Table 1**). On the contralateral side, the average number of cells per 400-fold field was 54.5 ± 3.5, whereas average apoptotic index was 4.35%.

Solitary TUNEL-labeled bodies in the form of small granules of different sizes and dense apoptotic bodies were observed on the contralateral side (**Figure 1B**). In our studies, TUNEL-positive cells with DNA fragmentation are shown in **Figure 1B–E**. After mechanical damage to the eye, distribution of TUNEL-positive elements in the optic nerve was uneven. TUNEL-positive cells were distributed on the damaged side and the number of TUNEL-positive cells was highest in the area of injury (**Figure 1D**). Intense peroxidase labeling of the nuclei of apoptotic cells shows signs of DNA fragmentation. Dark peroxidase labeled granules (apoptotic bodies) sometimes formed homogeneous conglomerates (**Figure 1D**, **E**). These structures were located at the site of the nucleus, evenly distributed in the cytoplasm, either shifted to the cytoplasmic membrane or grouped with one of the poles of the cell soma. For TUNEL-positive cells characterized by the presence of intact cell membrane around them with no foci of inflammatory infiltration, they sometimes exhibit an intense labeling of fibers in the optic nerve (**Figure 1F**). This effect arises from the rupture of karyolemma of the major damaged retinal cells, TUNEL-labeled fragmentation of chromatin in the cytoplasm, followed by its spread to some distance as a result of anterograde transport.

At 2 days after injury, we found that there were a large number of type I and type II cells that migrated on the ipsilateral side (**Figure 1C**). These cells formed longitudinal migratory flows (**Figure 1C**), surrounded by type III cells, and the number of which was also significantly increased. The average number of cells on the ipsilateral side was 2.28 fold greater than that on the contralateral one. The number of cells on the ipsilateral and contralateral sides was 54.5 and 124.5 per visual field, respectively (**Figure 1H**).

Along with the patterns of cell migration on the ipsilateral side, we observed massive accumulation of apoptotic bodies and numerous TUNEL-labeled cells (**Figure 1D**, **H**). The average sizes of nuclei stained with methyl green in regions of localization of TUNEL-labeled cells on the ipsilateral and contralateral sides were 5.3 ± 0.7 / 3.9 ± 0.5 μm respectively and the average size of apoptotic bodies were 5.9 ± 0.9 / 3.9 ± 0.5 μm respectively. The average number of apoptotic bodies per visual field on the contralateral and ipsilateral sides was 2.5/22.5 elements, respectively (**Figure 1H**). Patterns of cell degranulation representing the earlier stages of the apoptotic process and TUNEL-labeled fragments of degranulated chromatin were detected along with apoptotic crescents-like bodies (**Figure 1E**). A significantly increased number of cells were observed in the regions separating the individual fiber optic bundles – mesaxones (epineurium) (**Figure 1F**). In these regions, we also observed TUNEL-labeled apoptotic cells (**Figure 1F**). Along with the TUNEL-labeled cells on the ipsilateral side, portions of TUNEL-labeled fibers (**Figure 1G**) were observed. The ratio of apoptotic indices on contralateral and ipsilateral sides at 2 days after mechanical injury was 4.3/25.7%, respectively (**Figure 1I**).

Localization of PCNA in damaged optic nerve of trout 1 week after injury

To evaluate cell proliferative activity in the injured optic nerve, PCNA immunolabeling was performed at 1 week after injury. High cell proliferative activity was observed in the ipsilateral optic nerve (**Figure 2A**). Types II, III and IV cells were identified among PCNA-ip cells, and PCNA was also localized in type I migrating cells (**Figure 2A**, **B**). The staining intensity of PCNA was different in different types of cells (**Figure 2A**, **B**). PCNA-ip cells were unevenly

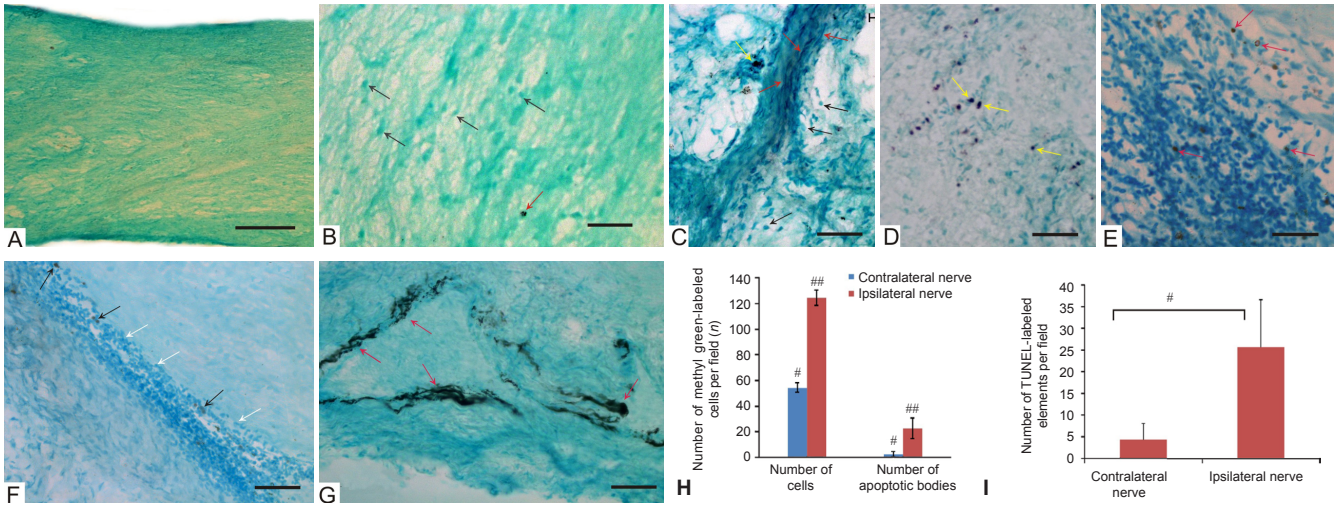

Figure 1 Morphological structure and apoptosis in the optic nerve of trout *Oncorhynchus mykiss*.
(A) General view of the contralateral optic nerve. (B) Cells (black arrows) and TUNEL-labeled granules (red arrow) in the contralateral nerve. (C) Patterns of cell migration (type I cells shown by black arrows, type II cells – red arrows, apoptotic bodies - yellow arrows) in the ipsilateral optic nerve. (D) Accumulation of apoptotic bodies (yellow arrows) in the proximal ipsilateral optic nerve. (E) A large cluster of types III and IV cells (red arrows) in mesaxons of ipsilateral optic nerve, red arrows indicate the different types of TUNEL-labeled elements. (F) General view of the proximal portion of the ipsilateral optic nerve, white arrows show type I migrating cells, and black arrows indicate TUNEL-labeled apoptotic bodies. (G) TUNEL-labeled fibers in the proximal ipsilateral optic nerve (red arrows). Immunoperoxidase TUNEL labeling in combination with methyl green staining. Scale bars: 200 μm (A) and 50 μm (B–G). (H) The number of cells stained with methyl green and TUNEL-labeled cells (mean ± SEM) per visual field in contralateral and ipsilateral nerves ($n = 5$ in each group; #$P < 0.05$, ##$P < 0.001$, *vs.* ipsilateral and contralateral nerves). (I) Number of TUNEL-labeled elements per visual field in the contralateral and ipsilateral nerves; *post hoc* Tukey's test was used to determine significant differences in contralateral and ipsilateral nerves.

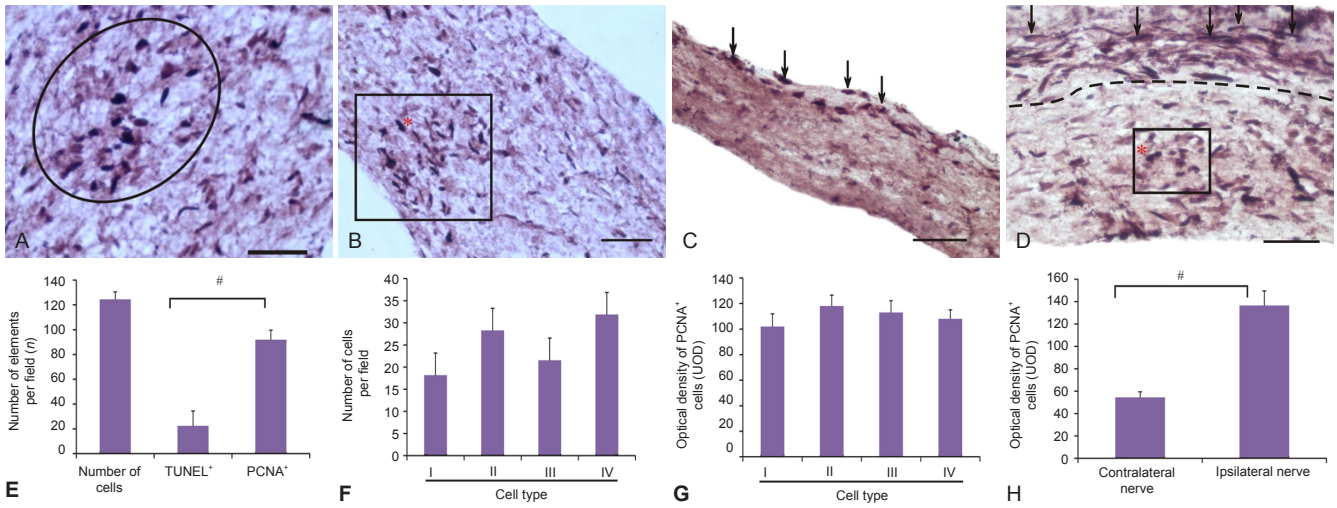

Figure 2 Localization of proliferative cell nuclear antigen (PCNA) in damaged optic nerve of trout 1 week after optic nerve injury.
(A) Clusters of intensely labeled type II and III cells (contoured by oval) in the deep layers of the damaged optic nerve. (B) Accumulation of immunopositive type I cells (contoured by square) in the surface layers of the damaged nerve, a red asterisk here and in figure D shows cells where mitosis was finished. (C) Migratory stream of moderately labeled cells in the superficial layers of optic nerve (shown by black arrows). (D) Stratification of migrating and moderately PCNA-labeled type I cells (indicated by black arrows) and highly immunopositive type IV cells (contoured by square), the area of migration is limited by dotted lines. Scale bars: 50 μm for A–D. (E) Number of TUNEL$^+$, PCNA-immunopositive (PCNA$^+$) elements and cells stained by methyl green per visual field in damaged nerve ($n = 5$ in each group; #$P < 0.05$). (F) Number of PCNA$^+$ cells of types I–IV in damaged optic nerve (mean ± SEM). (G) Optical density of PCNA immunolabeling in cells of types I–IV in damaged optic nerve (mean ± SEM). (H) Number of PCNA$^+$ cells in contralateral and ipsilateral nerves per 400-fold visual field; *post hoc* Tukey's test was used to determine significant differences in contralateral and ipsilateral nerves ($n = 5$ in each group; #$P < 0.05$).

distributed, and types III and IV cells often accumulated locally (**Figure 2A**) and type II cells also formed a zone with increased PCNA staining (**Figure 2B**). Type III migrating cells arranged into longitudinal rows in each layer of superficial optic nerve fiber (**Figure 2B**). In this case, some cells had clearly distinguishable PCNA-negative central area, and PCNA activity was high (**Figure 2C**). However, in some cases it was possible to divide the layers containing a large amount of PCNA-ip type I cells, form a surface migration flows and the deeper layers of the optic nerve, containing type IV PCNA-ip cells (**Figure 2D**). The ratio of PCNA-ip cells to apoptotic cells per visual field is shown in **Figure**

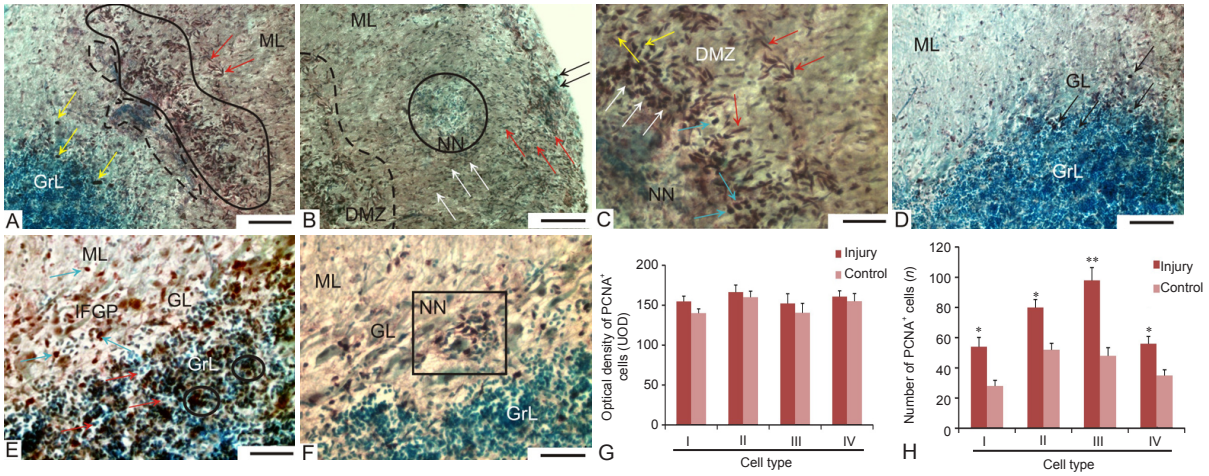

Figure 3 Localization of proliferative cells nuclear antigen (PCNA) in trout cerebellum 1 week after optic nerve injury.
(A) PCNA-immunopositive ($PCNA^+$) cells in the cerebellar dorsal matrix zone (DMZ) (delineated by a solid line), the accumulation of PCNA-immunonegative ($PCNA^-$) cells under the DMZ delineated by the dotted line, yellow arrows show intensively labeled oval cells in the granular layer (GrL), red arrows show rod-shaped migrating cells. (B) Dorsal part of the molecular layer (ML) of the cerebellum. Accumulation of $PCNA^-$ cells is delineated by circle, black arrows indicate the $PCNA^-$ tangentially migrating cells, red arrows point to $PCNA^-$ small round cells, white arrows indicate weakly labeled radially migrating cells, and NN represents neurogenic niche. $PCNA^+$ cells in the cerebellar DMZ are delineated by dotted line. (C) Cellular composition of DMZ. Type I cells are shown by red arrows, type II cells by yellow arrows, type III cells by blue arrows, and type IV cells by white arrows. (D) Ventral part of cerebellar body. Black arrows show $PCNA^+$ cells in molecular (ML), ganglionic (GL) and granular layers. (E) Infraganglionic plexus (IFGP) in dorsal part of the cerebellum. Blue arrows show the $PCNA^+$ cells in IFGS, red arrows point to $PCNA^-$ cells in GrL, ovals delineate a cluster of $PCNA^+$ cells in the granular layer. (F) Fragment of ganglionic layer containing neurogenic niche (contoured by square). Peroxidase PCNA immunolabeling on transversal brain sections *in situ*. Scale bars: 100 μm (A, B, D) and 50 μm (C, E, F). (G) Optical density of PCNA labeling in types I–IV cells in cerebellar DMZ (mean ± SEM). (H) Number of $PCNA^+$ types I–IV cells in cerebellar DMZ; Student's *t*-test was used to determine significant differences in control animals and animals after injury ($n = 5$ in each group; $^*P < 0.05$, $^{**}P < 0.001$, *vs.* control group). UOD: Units of optical density.

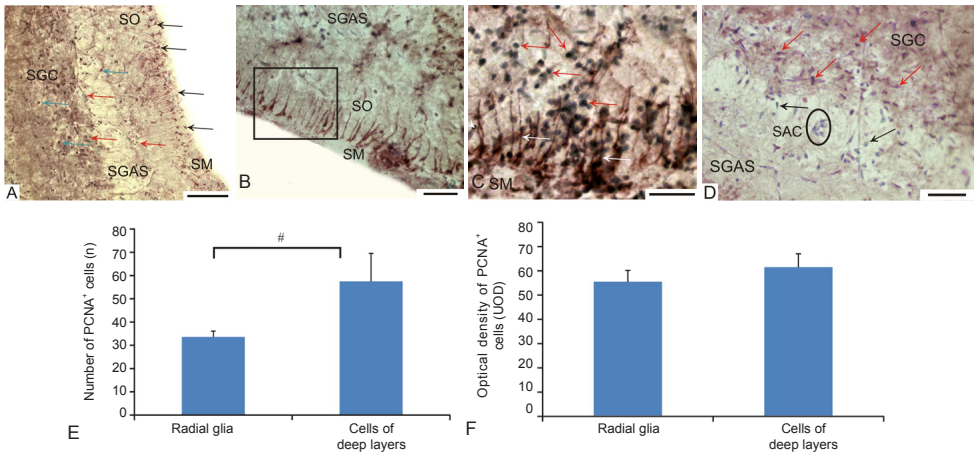

Figure 4 Localization of proliferative cell nuclear antigen (PCNA) in the potic tectum of trout 1 week after optic nerve injury.
(A) General view of optic tectum. Black arrows show PCNA-immunopositive ($PCNA^+$) cells of radial glia, blue arrows show $PCNA^+$ cells in deep layers, red arrows point to PCNA-immunonegative ($PCNA^-$) cells. (B) Radial glia (contoured by square) in *stratum marginale* (SM) of optic tectum. SO: *Stratum opticum*. (C) $PCNA^+$ radial glia (white arrows) and $PCNA^-$ cells (red arrows) at high magnification. (D) $PCNA^+$ cells (red arrows) in *stratum griseum et album superficiale* (SGAS), *stratum griseum centrale* (SGC), *stratum album centrale* (SAC), $PCNA^-$ cells (black arrows); cell cluster forming the neurogenic niche is contoured by oval. (E) Number of $PCNA^+$ elements: radial glial cells and immunopositive cells in the deep layers of optic tectum. Tukey's *post-hoc* test was used to determine significant differences in radial glia cells and immunopositive cells in deep layers. Error bars represent SEM ($n = 5$; $\#P < 0.05$). (F) Optical density of PCNA-labeling in radial glia and cells in deep layers of optic tectum (mean ± SEM). UOD: Units of optical density.

2F. The proportion of PCNA-immunonegative (in) cells in types I–IV cells is shown in **Figure 2F** The densitometric data of PCNA immunolabeling for cells of each type are shown in the diagram (**Figure 2G**). In types I–IV cells, we observed a wide range of OD in PCNA immunolabeling (**Table 1**). At 1 week after injury, the ratio of PCNA-ip cells on the contralateral optic nerve was significantly different from that on the ipsilateral side ($P < 0.05$; **Figure 2H**), and on the ipsilateral side, we observed more than 3 fold increase in the proliferative activity of cells.

Cellular response in the trout brain 1 week after optic nerve injury

At 1 week after optic nerve injury, the proliferative activity of

Table 1 Morphological parameters (mean ± SEM) and optical density of proliferating cell nuclear antigen-immunopositive ($PCNA^+$) optic nerve cells after stab wound injury of trout eyes

			Optical density of $PCNA^+$ cells (units of optical density)	
Cell type	Large diameter (μm)	Small diameter (μm)	Min.	Max.
I (large)	12.1±0.8	5±0.4		
II (elongated)	8.4±0.2	4.2± 0.5	108	124
III (round)	8.6±0.3	6.1±0.3	107	118
IV (small)	6.9±0.06	5±0.02	97	120

Table 2 Parameters of trout brain cells (mean ± SEM) in suspension and conglomerates after 1 and 2 days of culture (according to classification of Arevalo et al. (1995)).

	1 day suspension		1 day conglomerates		2 day suspension		2 day conglomerate	
Cell type	Size of cells (μm)	Percentage (%)	Size of cells (μm)	Percentage (%)	Size of cells (μm)	Percentage (%)	Size of cells (μm)	Percentage (%)
II	25.6±4.6/24.4±4.7	12.3	21.5±2.6/16.7±1.3	4.7	21.7±0.8/20.5±1.7	5.4	22.3±2.9/21.6±2.6	5.7
III	17.3±1.7/16±2.3	16.4	16.3±1.3/15.2±2.5	19	16.8±1.2/15.7±1.3	17.8	16.2±1.3/14.5±0.8	27.6
IV	12.3±1.3/11.3±1.5	58.7	12.3±1.4/11±0.9	23.8	12.5±1.5/11.3±1.6	52	11.1±1.3/10±1.3	27.8
V	8.9±0./8.1±0.8	12.3	7.6±1/6.9±1	52.3	8.4±1.2/7.8±1.4	24.6	8.3±1.1/7.6±1.3	38.8

cells in the cerebellum and the optic tectum was determined by PCNA immunoreactivity on histological brain sections.

Localization of PCNA in the cerebellum

PCNA immunoreactivity was found in the dorsal and ventral area of cerebellar body. In the dorsomedial region of the cerebellum, we observed large clusters of PCNA-ip cells forming dorsal matrix zone (**Figure 3A**). In the dorsal matrix zone, a lot of cells migrated in radial and tangential modes (**Figure 3B**). At the dorsal level of molecular layer, radially migrating cells were dominated; at the superficial level of molecular layer, we identified tangentially migrating cells (**Figure 3B**). High-density distribution of PCNA-in cells was observed near the PCNA-ip cells in the dorsal matrix zone (**Figure 3B**). Such accumulation of PCNA-ip cells with irregular shape was also observed directly under the dorsal matrix zone (**Figure 3C**). We believe that this cell formation is a regional neurogenic niche, formed as a result of traumatic exposure. In the molecular layer of the dorsomedial part of cerebellar body, we also observed round PCNA-in cells. The density of their distribution increased in the dorsal direction (**Figure 3B**). PCNA-ip cells in the dorsal matrix zone included highly labeled oval cells (perikaryon size 8.3 ± 0.9/6.4 ± 1.4 μm) and elongated, fusiform and/or rod-shaped cells (soma size 10.5 ± 0.5 / 6.9 ± 1.2 μm) (**Figure 3C**). In the cerebellar ventral region, the concentration of PCNA-ip cells was much lower (**Figure 3D**). Separate PCNA-immunopositive parenchymal cells were identified in the molecular layer (**Figure 3D**). In the superficial area of the granular layer we observed single small accumulation of PCNA-ip parenchymal cells, whose size was 7.4 ± 1.6 / 5.7 ± 0.9 μm. PCNA-ip cells were often found among granular cells. From dorsal side of granular layer, the number of PCNA-ip cells was much higher (**Figure 3D**). In the infraganglionic plexus, small parenchymal PCNA-ip cells were found (**Figure 3E**). Sometimes, small clusters of both PCNA-ip and -in cells were also identified in the territory of infraganglionic plexus (**Figure 3F**). We believe that these clusters represent regional neurogenic niches, proliferative activity in which was induced by mechanical trauma. Data about OD of PCNA labeling of different cell types in the dorsal matrix zone and quantifying PCNA-ip cells in the cerebellum are shown in **Figure 3G**, **H**. The OD of immuno-labeling after damage increases slightly in all cell types (**Figure 3G**). At 1 week after mechanical damage, the number of PCNA-labeled types I, II and IV cells in the dorsal matrix zone was significantly increased compared with controls ($P < 0.05$) and the increase in type III cells was highly significant ($P < 0.001$; **Figure 3H**).

Localization of PCNA in the optic tectum

After mechanical eye injury in an adult trout, numerous immunopositive cells were observed in the *stratum griseum et album superficiale* (SGAS), *stratum griseum centrale* (SGC), *stratum album centrale* (SAC), and *stratum griseum periventriculare* (SPV; **Figure 4A**, **D**). The sizes of PCNA-ip cells ranged from 6.2/3.4 μm (minimal) to 9.5/6.1 μm (maximal). The average size of PCNA-ip cells was 7.8 ± 1.1 / 4.9 ± 0.9 μm. In *stratum marginale* of tectum, PCNA-ip radial glial cells were identified (**Figure 4A**, **B**), the sizes of bodies in radial glia cells ranged from 6.7/5.1 μm (minimal) to 9.5/8 μm (maximal). The average size of PCNA-ip radial glia cells was 8.4 ± 1.2/6.1 ± 1.3 μm. The density of PCNA- immunopositive radial glia was relatively low and it was 33 ± 7 cells per visual field at 400-fold magnification (**Figure 4C**). The ratio of PCNA-ip radial glia in marginal layer and cells in the inner layers of the optic tectum are shown in **Figure 4E**. The OD of PCNA labeling in radial glial cells was varied: highly immunolabeled cells had 114.5 OD units and less intensely labeled cells had 104.4 OD units. In the deep layers of the optic tectum, the level of OD in PCNA-ip cells was higher than that in radial glia (**Figure 4F**). The maximal level of

PCNA labeling in cells of the optic tectum was 127.7 OD units , and the minimal was 116.2 OD units .

Evaluation of proliferative potential of trout brain cells *in vitro*

During culture, small fractions of cells adhered on the surface of culture dish and formed a monolayer fraction. Some of these cells began to form outgrowths (**Figure 5A**). The greater proportion of the cells remained in suspension (**Figure 5B–D**). Investigation of the cells in suspension revealed that pretreatment of brain cells with trypsin or collagenase in different modes and conglomerates tended to form (**Figure 5C**, **D**). Analysis of the cellular composition of conglomerates revealed that some of them were composed of isometric elements, which may be the descendants of a single cell and therefore represent typical neurospheres (**Figure 5E**). Other types of conglomerates were composed of heteromorphic elements and were apparently formed for the second time after changes in the surface properties and the adhesiveness of cells during preparation of the primary cultures (**Figure 5F**). The suspension fractions contained types II–V cells, according to above-described classification. Parameters of cells in suspension and conglomerates during 1–2 days of culture are shown in **Table 2**. Morphometric analysis of cell conglomerates as observed in suspension showed that the average size of these conglomerates was 42.7 ± 13.7 / 28.9 ± 9.2 μm after 1 day of culture. After analyzing the cellular composition of conglomerates, we found that the predominant cell types are small type V cells (**Table 2**). Mitosis was observed after 1 day of culture, and the average size of cells in mitosis was 16.6 ± 0.4 / 8.8 ± 0.2 μm. Mitosis was detected in type V isometric cells, with a diameter of about 8 μm. On the second day of culture, the ratio between the fraction of cells in suspension and the cells in the conglomerate differed from that on the first day.

Parameters of cells of different types in a suspension and conglomerates fractions are shown in **Table 2**. The average size of cell conglomerates on the 2nd day of culture was 50.7 ± 14.3 / 36 ± 10.3 μm. The number of different types of cells in conglomerates in suspension after 1–2 days of culture is shown in **Figure 5G**. A few type V cells with the diameter of 7.8 ± 2.1 / 7.3 ± 2.1 μm formed a monolayer. On the 4th day of culture, the typical neurospheres with diameters ranging from 23.04 / 20.74 μm to 72.09 / 55.75 μm were composed of type V isometric cells (**Figure 5E**). All cells in the neurospheres were of round shape with the same diameter of the transparent light cytoplasm (**Figure 5E**). The average diameter of neurospheres was 45.49 ± 16.8 / 33.3 ± 10.3 μm. Along with neurospheres, we also observed heterogeneous cell aggregates, which were present in the composition of one type II or type III large cell and several type IV or type V small cells (**Figure 5E**) in suspension fractions. Such conglomerates were considered as temporary cell clusters, which along with transparent living cells had dark dead cells. During this period, in monolayer, we also identified single cells (size 12.7/ 11.8 μm) without outgrowths. Type IV cells with the diameter of 11.3 ± 0.3 / 10.1 ± 0.6 μm and a few large type II cells with the diameter of 24.7 μm were observed in suspension.

Evaluation of proliferative activity in suspension fraction of trout brain cells

After 4 days of culture, cells in the brain of trout were analyzed for immunoperoxidase labeling of PCNA. The results of immunohistochemical labeling showed that PCNA-immunopositivity was present in type IV and type V cells (**Figure 6A**, **B**). Type V PCNA-ip cells, accounting for 84.7%, had a diameter of 6.9 ± 1.5 / 5.8 ± 1.3 μm and type V cells, accounting for 15.3%, had a diameter of 11.6 ± 1.1 / 9.2 ± 1.7 μm. Among type V cells, we identified a small subpopulation of cells with a diameter less than 6 μm and the average diameter of these cells was 5.2 ± 0.4 / 4.7 ± 0.4 μm. These cells accounted for one third of all type V cells (**Figure 6C**). Most of small type IV and V cells had two levels of PCNA immunoreactivity: the high level with the OD of immnolabeled precipitates in cells being 146,6 ± 5,7 OD units and the low level with the OD of immnolabeled precipitates in cells being 123.4 ± 8.2 OD units (**Figure 6D**). Strong PCNA activity was detected in cells with the diameter of 8.3 / 7.8 μm; frequency of densely labeled cells per visual field was low and accounted for no more than 5–6 elements (**Figure 6A**). Occasionally, we encountered PCNA-ip small cell clusters, which consisted of 2–3 cells and were densely labeled, and the remaining cells were less intensely labeled (**Figure 6B**). In small type V cells, the level of optical density was 118.8 ± 3.7 OD units.

Discussion

Proliferation and apoptosis of cells in the trout optic nerve after optic nerve injury

We detected the apoptosis and proliferative activity of cells in trout optic nerve after mechanical damage of the eye. These processes prevailed on the ipsilateral side, since the number of TUNEL-labeled cells was 6.5 times and the number of proliferating cells was 2.8 times greater than those on the contralateral side. The optic nerve is formed by axons of RGS and glial cells (astrocytes and Schwann cells) and macrophages / microglia, which are activated in response to the damaging effects. Analysis of morphological parameters of the cells in the trout's optic nerve allows distinguishing four types of cells. After damage to the optic nerve, apoptotic response was registered, and mass patterns of cell migration were found. The maximal concentration of apoptotic bodies was detected in the areas of mass clumps of cells. It is probably indicative of massive cell death in the area of high phagocytic activity of macrophages / microglia. Patterns of cell migration identified on 2 days after injury also indicate an increase in the cell flow directed to the area of injury. After damaging the eyes, we identified the patterns of apoptosis equally as the presence of high cell density zones and cell migration patterns in the optic nerve. We assume that such areas in optic nerve may correspond to the zones of reactive gliosis occurring in response to injury. We believe that as a result of the damaging effects, a heterogeneous cell population of optic nerve involving astrocytes, Schwann cells and resident fibroblastic cells appeared among apoptotic cells.

In studies on goldfish, in the optic nerve of adult fish Pax2-positive and Pax2-negative cells are present (Parrilla et

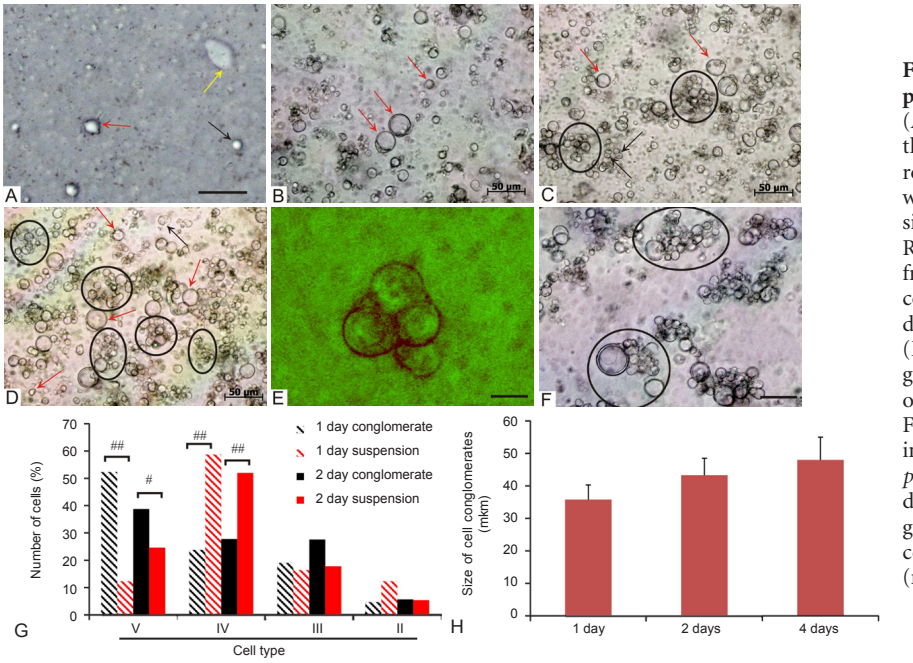

Figure 5 Phase contrast monitoring in primary culture of trout brain cells.
(A) Cells in monolayer; colored arrows indicate the different types of cells: big cell (yellow arrow), cells with outgrowth (red arrow) and cell without outgrowth (black arrow). (B) Suspension fraction of brain cells after 1 day of culture. Red arrow shows single cells. (C) Suspension fraction of cells on the 2nd day of culture. Ovals contour cell conglomerates, and red arrows indicate single cells. (D) On the 4th day of culture. (E) General view of neurospheres. (F) Heterogeneous conglomerates of cells in suspension on the 4th day of culture. Scale bars: 50 μm (A–D, F), 10 μm (E). (G) Number of types II–V cells in suspension after 1–2 days of culture. Tukey's *post-hoc* test was used to determine significant differences in number of cells ($n = 7$ in each group; $\#P < 0.05$, $\#\#P < 0.001$). (H) Size of cell conglomerates after 1, 2 and 4 days of culture (mean ± SEM).

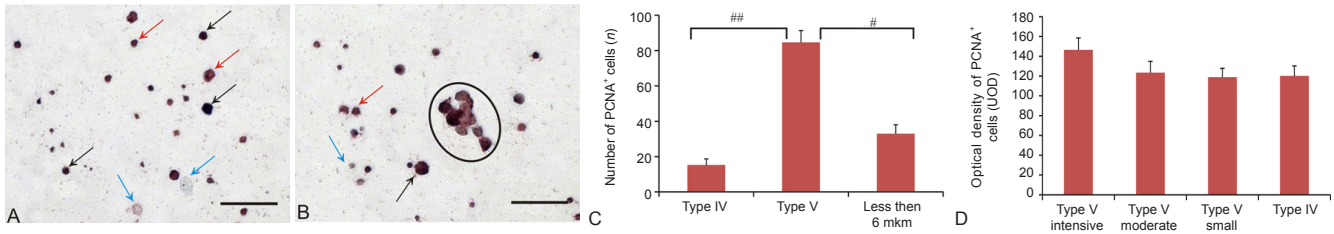

Figure 6 Proliferative cell nuclear antigen (PCNA) labeling of trout brain cells after 4 days in primary culture.
(A) Highly active PCNA-immunopositive ($PCNA^+$) cells (black arrows), moderately active $PCNA^+$ cells (red arrows) and PCNA-immunonegative cells (blue arrows); (B) Conglomerate of highly and moderately labeled $PCNA^+$ cells (contoured by oval); arrows represent the same cells as in A. Scale bars: 50 μm (A, B). (C) Tukey's *post-hoc* test was used to determine significant differences in number of $PCNA^+$ cells. Error bars represent (mean ± SEM, $\#P < 0.05$, $\#\#P < 0.001$). (D) Optical density of $PCNA^+$ cells (mean ± SEM).

al., 2009). Pax2 is a well known transcription factor which participates in optic nerve development. It assures the correct arrival and package of the newly formed retinal axons and the adequate differentiation of the newly formed glial cells. Pax2 protein expression is continuous throughout adult life in the goldfish optic nerve. It has been proposed that optic nerve head astrocytes, including Pax2 positive cells, come from migrating astrocyte precursors of the retina during development (Chu et al., 2001; Yang and Hernandez, 2003). However, Macdonald et al. (1997) suggested that Pax2 positive cells in the zebrafish optic nerve originate from the optic stalk cells expressing this transcription factor during the development.

Double labeling of Pax2 and PCNA in the optic nerve of goldfish showed that few proliferating Pax2-positive/PCNA-positive cells were observed in the optic nerve head. In the lateral intraorbital zone, these cells were located in the area that forms a boundary between the photoreceptor segments and the optic nerve (Parrilla et al., 2009).

After crushing optic nerve in goldfish, a significant increase of Pax2-ip astrocytes was revealed, but pattern of distribution of Pax2-ip cells was similar to that in control (Parrilla et al., 2013). In contrast to adult intact goldfishes, Zn8-immunolabeling revealed a high amount of regenerating axons located in the growing edge close to the optic chiasm, but also in mature regions of the optical nerve head. Pax2-ip astrocytes were longitudinally arranged to the Zn8-positive growing axons from the growing edge (Parrilla et al., 2013).

According to Parrilla et al. (2013), after crushing the optical nerve in goldfish, during 7 to 60 days after injury, the number of $PCNA^+/Pax2^+$ cells significantly increased compared with control. These $Pax2^+/PCNA^+$ astrocytes were located close to the optic chiasm among the RGC axons. Similar results were obtained after double labeling of PCNA / S100 (Parrilla et al., 2013).

Astrocytes have been shown to play an important role during the process of regeneration which allows the fish visual system to completely regenerate, but this does not occur in mammals (Garciá and Koke, 2009). In teleosts, the $Pax2^+$ astrocyte population and pax2a gene expression are modified in the optic nerve head after a peripheral growth zone cryolesion when the regenerating RGC axons reach the optical nerve head (Parrilla et al., 2013).

Significant progress in the understanding of successful regeneration after amputation of caudal part of spinal cord

has been made in the study of electric fish *Apteronotus leptorhynchus* (Zupanc, 2009). In this study, successful recovery of the lost fragments of the spinal cord along with the amputated part of caudal fin has been demonstrated. One of the initial stages of the repair process after injury is the rapid destruction of damaged cells by apoptosis. According to Zupanc (2009), the first apoptotic cells appear in an area of damage during 5 minutes after injury; and then the number of apoptotic elements increases gradually, reaching a maximal level after few hours. On the second day, the number of apoptotic cells in the spinal cord of *A. leptorhynchus* is gradually reduced, reaching the background level approximately after 3 weeks. During this period, only some cells undergo necrosis. Elimination of damaged cells by apoptosis in fish brain differs significantly from that in the mammalian brain (Vajda, 2002). In the mammalian brain, necrosis is the major type of elimination of damaged cells after injury (Liou et al., 2003). Apoptosis is also present in a small number of cells adjacent to the injury area. Necrosis prevails in mammalian brain and is one of the causes of secondary inflammation in damage zone (Kerr et al., 1995). This in turn causes a further increase in necrotic response and formation of larger cavities without cells. These cavities are usually limited by area of reactive astrocytes, creating both mechanical and biochemical barriers that impede the growth of nerve fibers and cell migration in the damage zone. In contrast, for the apoptotic cells, overall compression and condensation of the nucleus and the formation of vesicles which are then deleted by macrophages/microglia are the main characteristics (Elmore, 2007). Similar changes in the damaged optic nerve of trout were observed 2 days after injury. Initially, the number of phagocytes was negligible in damaged area, but 3 days after injury the number of macrophages began to increase in the injury area, and in adjacent areas (Nagamoto-Combs et al., 2007). These data are entirely consistent with our observations on the optic nerve of trout. The main effects of necrosis, associated with inflammation response of the surrounding tissue are completely absent in apoptosis. Thus, the prevalence of processes of "clean" cell death for the destruction of damaged cells is a critical feature underlying the regenerative capacity of the adult fish brain.

Investigation of proliferative activity in damaged optic nerve 1 week after injury showed the presence of large number of cells in state of proliferation. In optic nerve, areas of increased cell density contained oval types II and III cells. Elongated cells, located in the superficial layers of nerve, were obviously in a state of migration. PCNA labeling allows identifying the cells, where the expression of additional DNA polymerase δ occurs. These cells were in S-phase of mitosis. PCNA expression in the cells is maintained for 24 hours after mitosis (Wulliman and Puelles, 1999).

Monitoring of proliferating and migrating cells in damaged optic nerve showed that actively proliferating cells form restricted areas of increased density of cell distribution, but migratory cells are typically arranged among superficial optic fibers. Densitometric analysis of PCNA labeling revealed that types II and III oval cells have a high OD, whereas OD in type I large cells and type IV small cells was lower to 22–30%.

According to Bravo and McDonald Bravo (1987), for the post-mitotic cells, PCNA labeling is characterized by 30% reduced activity. This suggests that in damaged optic nerve, proliferating cells (glial cells) and post-mitotic cells were present as shown by PCNA labeling, but PCNA activity was reduced compared with that in cells in the state of proliferation. We assume that the proliferating cells presented by Schwann cells and/or astrocytes are involved in the formation of post-traumatic reactive gliosis. However, along with astrocytes we found large migrating cells, probably belonging to the population of resident macrophages. Types I and IV small poorly PCNA-labeled cells are elements of microglia. We suggest that types I and IV cells may be elements of immune system and are mobilized as a result of damaging effects. Ratio of PCNA-ip cells in contralateral and ipsilateral trout optic nerve 1 week after injury was significantly different. In damaged optic nerve, we found that more than 3-fold increase of proliferative activity in different types of cells. We believe that such an increase in volume of cells in the optic nerve on the ipsilateral side is attributable to the proliferation of glial cells and microglia and the migration of resident macrophages of the adjacent connective tissue.

Proliferative response in the trout brain integration centers after mechanical eye injury

After stab-wound injury, proliferative activity was investigated in the cerebellum and optic tectum. The optic tectum is known to be the target of primary retinal projection. After mechanical eye injury, proliferative activity was found in the cerebellar dorsal matrix area, as well as in single parenchymal cells located in basal part of molecular layer, granular layer and infraganglionic plexus. In this study, we identified PCNA-in clusters of activated cells in regional neurogenic niches. Proliferative activity was found in the dorsal matrix zone of cerebellum, which was described in the cerebellum of zebrafish (Grandel et al., 2006) and *Apteronotus leptorhynchus* (Zupanc et al., 2005). In the brain of zebrafish, during a 30 minute period, about 6,000 cells formed, which correspond to 0.2% of total cells in the brain (Hinsch and Zupanc, 2007). Quantitative studies on the cerebellum *Apteronotus leptorhynchus* showed that during a 2 hour period, about 100,000 cells formed, which correspond to 0.06% of total brain cells (Zupanc and Horschke, 1995). After traumatic impact, three types of PCNA-ip cells were found in the trout cerebellum. PCNA-ip cells contained highly immunoreactive oval cells (116 ± 4.5 OD units) and lowly immunoreactive elongated cells (103 ± 3.2 OD units). In this study, several populations of intensively PCNA-labeled cells in different stages of mitosis were found in the dorsal matrix zone, and less intensely labeled cells were considered post-mitotic elongated elements, migrating in radial and tangential directions outside from the dorsal matrix zone towards damaged region. Another population of cells involved in the proliferative response of the CNS after mechanical damage represented PCNA-in cell clusters with high cell density. These cell clusters were observed above and below the dorsal matrix zone and in the infraganglionic plexus. We assume that these

clusters of PCNA-in cells are neurogenic niches activated after optic nerve injury. These observations are consistent with the data of Zupanc et al. (1996, 2005). According to Zupanc et al. (1996, 2005), neural stem cells (NSC) are in specific proliferative zones "neurogenic niches" located in the molecular layer. Descendants of proliferated cells migrate along specific routes in the granular layer, where they are distributed evenly (Candal et al., 2005; Zupanc et al., 2005). The third population is PCNA-ip cells arranged singly or in small clusters in the lower one third part of the molecular layer and granular layer.

The optic tectum is another sensory integration center in the trout brain. Earlier PCNA labeling for identification of proliferative activity of mesencephalic matrix zones was revealed in *Carassius carassius* (Margotta et al., 2002). It was found that PCNA labeling allows the identification of patterns of distribution of mitotically active cells in the brain that form morphogenetic fields - the matrix zones. Matrix zone labeled by PCNA in the mesencephalon, has also been identified in the adult sturgeon *Acipenser shrenkii* (Pushchina and Obukhov, 2011).

After mechanical eye injury in trout, PCNA immunopositivity was detected in radial glial cells, single parenchymal cells of inner layers and in the periventricular tectal region. It is known that the populations of radial glia in the brain of fish are not homogenous and include rapidly and slowly proliferating cells (Adolf et al., 2006).

We assume that after stab wound injury of trout optic tectum, proliferative activity was enhanced in slowly proliferating cells in radial glia. This assumption is based on data from densitometric analysis of PCNA activity in tectal radial glia cells. Compared with the density distribution of single parenchymal PCNA-ip cells in the deeper layers of the optic tectum, the density distribution of PCNA-ip cells in the radial glia was not high. We believe that after eye injury, only a part of radial glia population in the optic tectum proliferated. The OD of radial glia immunolabeling allows allocation of a few cells with high PCNA activity (114 OD units). We interpreted these cells as neuronal precursors (Malatesta et al., 2008) in the state of asymmetric mitosis that was previously set for radial glia cells (Noctor et al., 2004). Another more numerous population of radial glia in the trout optic tectum had 104 OD units; such cells we considered as post-mitotic cells. A large cluster of PCNA-ip cells were detected in the periventricular zone of caudal optic tectum, also found in other fish species (Extröm et al., 2001; Zupanc et al., 2005). PCNA immunopositivity in the trout optic tectum was mainly found in small cells. At 1 week after optic nerve injury, the proliferative activity was mainly found in the dorsal matrix zone of the cerebellum, radial glia and primary periventricular zone of the optic tectum, and some parenchymal cells. We identified the radial and tangential patterns of cell migration in the cerebellum, among which we detected PCNA-ip and -in elements. We identified PCNA-in neurogenic niches especially in the dorsal part of the cerebellum and in the optic tectum.

Our results showed that: (1) destroying the integrity of the eyes and injury to optic nerve head lead to intense proliferation and migration of cells in the optic nerve head region. We assume that optic nerve cells with proliferating reactive astrocytes arise in response to optic nerve injury. (2) Adjacent muscle fibers damaged by trauma are a source of regional macrophages involved in the neuroimmune interactions during the post-traumatic period. (3) As a result of combined mechanical eye injury and optic nerve crush in the sensory integration centers cerebellum and optic tectum, proliferative response occurred. In the dorsal part of the cerebellum in response to mechanical eye injury and optic nerve crush, we identified neurogenic niches and radial and tangential cell migration. The number of PCNA-labeled radial glia cells increased in the parenchyma and neurogenic niches of the optic tectum. These data indicate that crush of the optic nerve head can cause the proliferative response of cells in the matrix areas and activation of neurogenic niches.

Primary culture of trout brain cells

Primary culture of salmonid cells from various organs such as the heart CHH-1 (ATCC CRL 1680), ASH; kidney YNK, LTK; liver LTL; and gonads RTG-2 (ATCC CCL 55), RTO, RTF, ASO has been performed in different salmon species *Oncorhynchus keta* (Watanabe et al., 1978; Lannan et al., 1984), *Oncorhynchus masou* (Watanabe et al., 1978), *Oncorhynchus mykiss* (Wolf and Quimby, 1962), *Salmo salar* (Wolf and Mann, 1980), and *Salvelinus namaycush* (Cheng et al., 1993). Salmon embryo cells are most successfully cultured, because they survive well under the culture condition and are capable for further growth and development *in vitro* (Lannan et al., 1984; Fernandez et al., 1993; Larke et al., 2011). However, to the best of our knowledge, no studies have been reported on culture of salmonid brain cells and particularly on primary culture of adult salmon brain cells. Therefore, this study was the first to attempt to perform primary culture of adult trout brain cells. Cells from various organs of the trout, like gonads (Larke et al., 2011), kidneys (Andral et al., 1990), and muscle (Fernandez et al., 1993) had been cultured. Culture of trout cells under pathological conditions, such as hepatoma RTH-149 (ATCC CRL-1710) cell line (Andral et al., 1990) and nephroblastoma RTN (Wolf and Mann, 1980) has been reported. Culture of trout embryos RTE, RTE-2 (Fernandez et al., 1993) and young fry RTF-1 (Wolf and Mann, 1980) has been successfully conducted.

Results from this study showed that the linear volume of cell conglomerates increased with culture time. We also found that the sizes of conglomerates range from 33 / 19.9 to 99.6 / 62.7 μm on day 1 of culture and from 23 / 20.4 to 105 / 62.3 μm on day 4 of culture. This clearly illustrates the gradual linear increase in the size of conglomerates and gives the reason to conclude that the *in vitro* proliferation processes of cells of the CNS of adult trout can be recorded by cell culture. Findings regarding patterns of mitosis and of cells entering into differentiation processes and forming a monolayer suggest the utility of such primary culture systems for observing the process of proliferation and differentiation *in vitro*, which are otherwise difficult to be observed *in vivo*. Interestingly, after 4 days of culture, most of the cells were in

suspension while others remained in the form of adherence. We further confirmed that the majority of cells in suspension were proliferating but not dead and some of them conglomerates. We also observed higher proliferative activity in the suspension compared to in the form of adherence. In this study, we did not pay special attention to creating special conditions for the subsequent differentiation of cells in the monolayer, and therefore, we did not add specific growth factors to the growth medium. Significant proliferative activity was observed in cells in suspension and as part of conglomerates. Immunohistochemistry analysis of suspension cells showed that type IV small cells were in the proliferative state. Analysis of the cellular composition of conglomerates revealed that some conglomerates are formed by isometric elements, which may be the descendants of a single cell and, therefore, represent typical neurospheres in suspension. Detection of neurospheres, which we interpreted as descendants of stem cells, was confirmed by immunohistochemical labeling of PCNA. PCNA immunopositivity was found predominantly in single cells and small cells forming conglomerates. Unequal intensity of PCNA labeling of cells in the conglomerates in our opinion indicates heterochronic proliferation of these cell clusters. Thus, we consider the most intensely labeled cells as being able to direct the proliferation while cells with comparatively lesser intensity as the cells in which mitosis is complete. In trout brain cell suspension, we identified very small cells (less than 5 μm in size) with the highest activity of PCNA labeling. We believe that this type of cells are the most actively proliferated population of cells of the adult trout brain and maybe this type of cells may be located in the proliferative zones of adult trout brain.

According to Zupanc (2011), in adult fish brain new cells arise from precursor cells that have stem cell properties. Insulation like cells from the dorsal telencephalon and dorsal part of the cerebellum from electric fish *A. leptorhynchus* were investigated (Hinsch and Zupanc, 2006). In particular, after 3–4 days of culture, cells isolated from dorsal matrix area of the cerebellum and dorsal telencephalon of *A. leptorhynchus* can be transformed into different cell types (*e.g.*, particularly in GFAP-ip astrocytes, vimentin-positive cells, Hu-expressing cells and microtubule-associated protein 2 (MAP2) (2a + 2b)-ip neurons) by adding embryonic serum to the culture medium (Hinsch and Zupanc, 2006). After 3–4 days in culture, these cells give rise to neurospheres that grow through cell proliferation and reach diameters of as much as 140 mm within 3 weeks. The growth of neurospheres was enhanced by epidermal growth factor and basic fibroblast growth factor. According to Hinsch and Zupanc (2006), similar cells isolated from areas of the matrix zones of brain possess properties of multipotent differentiation as they can be transformed into different types of neurons, glia, and further retain the ability to proliferate.

In this study, we did not specifically isolate cells of the matrix areas of the brain, but culture of cells from the whole trout brain showed that cells retain much high capacity to proliferate. Perhaps one explanation for a significant proliferative potential in cultured trout brain cells is the lack of growth factors in the culture medium. The formation of two types of conglomerates, *i.e.*, heteromorphic and homogeneous, indicates the high proliferative potential of brain cells to successfully proliferate in the culture.

Thus, we isolated cells from the brain of trout and cultured them *in vitro* under the standardized conditions as described above. We observed formation of heteromorphic and isomorphic (neurospheres) conglomerates with high proliferation activity along with the cells in suspension. As shown earlier, neuronal regeneration is intimately linked to adult neurogenesis. Different species of fish examined thus far also generate new neurons constitutively, both in large numbers and in many regions of the adult CNS. Comparative analysis has suggested that adult neurogenesis is a primitive vertebrate trait (Zupanc, 2006). It is likely that the availability of all the cellular and molecular regulatory mechanisms necessary for the generation of new neurons in the intact CNS has greatly facilitated the repurposing of the cellular machinery for neuronal regeneration with only slight adaptive changes. A broad understanding of the biology of adult neurogenesis and neuronal regeneration will also facilitate the analysis of the selective pressures that have caused the loss of the regenerative potential during the evolution of mammals. We tend to further study the process of differentiation in these cultured cells and propose them to be used as a model system for further study of mechanism underlying adult neurogenesis in the salmonid fishes.

Author contributions: *EVP designed the study, prepared animal models, performed immunohistochemistry study, analyzed experimental data, and wrote the paper. SS performed cell culture and edited the paper. AAV and DKO also participated in paper writing and provided critical revision of the paper for intellectual content. All authors approved the final version of this paper.*

Conflicts of interest: *None declared.*

Plagiarism check: *This paper was screened twice using Cross-Check to verify originality before publication.*

Peer review: *This paper was double-blinded and stringently reviewed by international expert reviewers.*

References

Adolf B, Chapouton P, Lam CS, Topp S, Tannhäuser B, Strähle U, Götz M, Bally-Cuif L (2006) Conserved and acquired features of adult neurogenesis in the zebrafish telencephalon. Devel Biol 295:278-293.

Andral R, Hurard C, Elziere-Papayanni P, Vivares CP (1990) Establishment and characterization of a rainbow trout kidney cell-line, RTK Montpellier. In: Pathology in Marine Science (Perkins FO, Cheng CC, eds), pp33-42. San Diego: Academic Press, USA.

Arévalo R, Alonso JR, García-Ojeda E, Briñón JG, Crespo C, Aijón J (1995) NADPH-diaphorase in the central nervous system of the tench (*Tinca tinca* L., 1758). J Comp Neurol 352:398-420.

Arvidsson A, Collin T, Kirik D, Kokaia Z, Lindvall O (2002) Neuronal replacement from endogenous precursors in the adult brain after stroke. Nat Med 8:963-970.

Bonfanti L, Strettoi E, Chierzi S, Cenni MC, Liu XH, Martinou J-C, Maffei L, Rabacchi SA (1996) Protection of retinal ganglion cells from natural and axotomy-induced cell death in neonatal transgenic mice overexpressing bcl-2. J Neurosci 16:4186-4194.

Bravo R, Macdonald-Bravo H (1987) Existence of two populations of cyclin/proliferating cell nuclear antigen during the cell cycle: association with DNA replication sites. J Cell Biol 105:1549-1554.

Callahan MP, Mensinger AF (2007) Restoration of visual function following optic nerve regeneration in bluegill (*Lepomis macrochirus*) x pumpkinseed (*Lepomis gibbosus*) hybrid sunfish. Vis Neurosci 24:309-317.
Candal E, Anadón R, DeGrip WJ, Rodríguez-Moldes I (2005) Patterns of cell proliferation and cell death in the developing retina and optic tectum of brown trout. Devel Brain Res 154:101-119.
Cheng L, Bowser PR, Spitsbergen JM (1993) Development of cell cultures derived from lake trout liver and kidney in a hormone-supplemented, serum-reduced medium. J Animal Health 5:119-126.
Chu Y, Hughes S, Chan-Ling T (2001) Differentiation and migration of astrocyte precursor cells and astrocytes in human fetal retina: relevance to optic nerve coloboma. FASEB J 15:2013-2015.
Elmore S (2007) Apoptosis: a review of programmed cell death. Toxicol Pathol 35:495-516.
Extröm P, Johnsson CM, Ohlin LM (2001) Ventricular proliferation zones in the brain of an adult teleost fish and their relation to neuromeres and migration (secondary matrix) zones. J Comp Neurol 436:92-110.
Fernandez RD, Yoshimizu M, Kimura T, Ezura Y (1993) Establishment and characterization of seven continuous cell lines from freshwater fish. J Aquat Anim Health 5:137-147.
Garcıá DM, Koke JR (2009) Astrocytes as gate-keepers in optic nerve regeneration—a mini-review. Comp Biochem Physiol A Mol Integr Physiol 152:135-138.
Germain F, Calvo M, de la Villa P (2004) Rabbit retinal ganglion cell survival after optic nerve section and its effect on the inner plexiform layer. Exp Eye Res 78:95-102.
Grandel H, Kaslin J, Ganz J, Wenzel I, Brand M (2006) Neural stem cells and neurogenesis in the adult zebrafish brain: origin, proliferation dynamics, migration and cell fate. Devel Biol 295:263-277.
Hinsch K, Zupanc GK (2006) Isolation, cultivation, and differentiation of neural stem cells from adult fish brain. J Neurosci Methods 158:75-88.
Hinsch K, Zupanc GK (2007) Generation and long-term persistence of new neurons in the adult zebrafish brain: a quantitative analysis. Neuroscience 146:679-696.
Humphrey MF, Beazley LD (1985) Retinal ganglion cell death during optic nerve regeneration in the frog *Hyla moorei*. J Comp Neurol 236:382-402.
Kato S, Devadas M, Okada K, Shimada Y, Ohkawa M, Muramoto K, Takizawa N, Matsukawa T (1999) Fast and slow recovery phases of goldfish behavior after transection of the optic nerve revealed by a computer image processing system. Neuroscience 93:907-914.
Kerr JF, Gobé GC, Winterford CM, Harmon BV (1995) Anatomical methods in cell death. In: Cell Death (Schwartz LM, Osborne BA, eds) pp1-27. San Diego: Academic. Press, USA. 1995.
Kishimoto N, Shimizu K, Sawamoto K (2012) Neuronal regeneration in a zebrafish model of adult brain injury. Dis Model Mech 5:200-209.
Lannan CN, Winton JR, Fryer JL (1984) Fish cell lines: establishment and characterization of nine cell lines from salmonids. In Vitro 20:671-676.
Larke WS, Swaminathan TR, Joy KP (2011) Development, characterization, conservation and storage of fish cell lines: a review. Fish Physiol Biochem 37:1-20.
Liou AK, Clark RS, Henshall DC, Yin XM, Chen J (2003) To die or not to die for neurons in ichemia, traumatic brain injury and epilepsy: a review on the stress-activated signaling pathways and apoptotic pathways. Progr Neurobiol 69:103-142.
Macdonald R, Scholes J, Strähle U, Brennan C, Holder N, Brand M, Wilson SW (1997) The Pax protein Noi is required for commissural axon pathway formation in the rostral forebrain. Development 124:2397-2408.
Mack AF (2007) Evidence for a columnar organization of cones, Muller cells, and neurons in the retina of a cichlid fish. Neuroscience 144:1004-1014.
Malatesta P, Appolloni I, Calzolari F (2008) Radial glia and neural stem cells. Cell Tissbue Res 331:165-178.
Margotta V, Morelli A, Gelosi E, Alfei L (2002) PCNA positivity in the mesencephalic matrix areas in the adult of a teleost, *Carassius carassius* L. Ital J Anat Embryol 107:185-198.
McCurley AT, Callard GV (2010) Time course analysis of gene expression patterns in zebrafish eye during optic nerve regeneration. J Exp Neurosci 4:17-33.
Merkulov AG (1969) Course of patologohistological techniques. Leningrad: Medicine. (in Russian).
Nagamoto-Combs K, McNeal DW, Morecraft RJ, Combs CK (2007) Prolonged microgliosis in the rhesus monkey central nervous system after traumatic brain injury. J Neurotrauma 24:1719-1742.
Noctor SC, Martínez-Cerdeño V, Ivic L, Kriegstein AR (2004) Cortical neurons arise in symmetric and asymmetric division zones and migrate through specific phases. Nat Neurosci 7:136-144.
Parrilla M, Lillo C, Herrero-Turrión MJ, Arévalo R, Aijón J, Lara JM, Velasco A (2013) Pax2+ as trocytes in the fish optic nerve head after optic nerve crush. Brain Res 1492:18-32.
Parrilla M, Lillo C, Herrero-Turrion MJ, Arévalo R, Lara JM, Aijón J, Velasco A (2009) Pax2 in the optic nerve of the goldfish, a model of continuous growth. Brain Res 1255:75-88.
Pushchina EV, Obukhov DK (2011) Processes of proliferation and apoptosis in the brain of the Amur sturgeon. Neurophysiology 43:271-286.
Rodger J, Goto H, Cui Q, Chen PB, Harvey AR (2005) cAMP regulates axon outgrowth and guidance during optic nerve regeneration in goldfish. Mol Cell Neurosci 30:452-464.
Scalia F, Arango V, Singman EL (1985) Loss and displacement of ganglion cells after optic nerve regeneration in adult *Rana pipiens*. Brain Res 344:267-280.
Vajda FJ (2002) Neuroprotection and neurodegenerative disease. J Clin Neurosci 9:4-8.
Watanabe M, Inukai N, Fukuda Y (2001) Survival of retinal ganglion cells after transection of the optic nerve in adult cats: a quantitative study within two weeks. Vis Neurosci 18:137-145.
Watanabe T, Kobayashi N, Sato Y, Ishizaki Y (1978) Continuous cell line derived from the kidney of yamame, *Oncorhynchus masou*. Bull Japan Soc Sci Fish 44:415-418.
Wolf K, Mann JA (1980) Poikilotherm vertebrate cell lines and viruses: a current listing for fishes. In Vitro 16:168-179.
Wolf K, Quimby MC (1962) Established eurythermic line of fish cells in vitro. Science 135:1065-1066.
Wulliman MF, Puelles L (1999) Postembryonic neural proliferation in the zebrafish forebrain and its relationship to prosomeric domains. Anat Embryol 329:329-348.
Wyatt C, Ebert A, Reimer MM, Rasband K, Hardy M, Chien CB, Becker T, Becker CG (2010) Analysis of the astray/robo2 zebrafish mutant reveals that degenerating tracts do not provide strong guidance cues for regenerating optic axons. J Neurosci 30:13838-13849.
Yang P, Hernandez MR (2003) Purification of astrocytes from adult human optic nerve heads by immunopanning. Brain Res Brain Res Protoc 12:67-76.
Zou S, Tian C, Ge S, Hu B (2013) Neurogenesis of retinal ganglion cells is not essential to visual functional recovery after optic nerve injury in adult zebrafish. PLoS One 8:e57280.
Zupanc GK (2006) Adult neurogenesis and neuronal regeneration in the teleost fish brain: implications for the evolution of a primitive vertebrate trait. In: The Evolution of Nervous Systems in Non-mammalian Vertebrates (Bullock TH, Rubenstein LR, Zupanc GK, Sîrbulescu RF, eds), pp485-520. Oxford: Academic Press.
Zupanc GK (2009) Towards brain repair: insights from teleost fish. Semin Cell Dev Biol 20:683-690.
Zupanc GK (2011) Adult neurogenesis in teleost fish In: Neurogenesis in the adult brain (Seki T, Sawa-moto K, Parent JM, Alvarez-Buylla A, eds), pp137-168. Tokyo: Springer.
Zupanc GK, Horschke I (1995) Proliferation zones in the brain of adult gymnotiform fish: a quantitative mapping study. J Comp Neurol 353:213-233.
Zupanc GK, Sirbulescu RF (2013) Teleost fish as a model system to study successful regeneration of the central nervous system. Curr Top Microbiol Immunol 367:193-233.
Zupanc GK, Hinsch K, Gage FH (2005) Proliferation, migration, neuronal differentiation, and long-term survival of new cells in the adult zebrafish brain. J Comp Neurol 488:290-319.
Zupanc GK, Horschke I, Ott R, Rascher GB (1996) Postembryonic development of the cerebellum in gymnotiform fish. J Comp Neurol 370:443-464.

Copyedited by Yang CG, Hu Y, Li HY, Li CH, Song LP, Zhao M